Acetone-Butanol-Ethanol Competitive Sorption Simulation from Single, Binary, and Ternary Systems in a Fixed-Bed of KA-I Resin

ARTICLE *in* BIOTECHNOLOGY PROGRESS · FEBRUARY 2015

Impact Factor: 2.15 · DOI: 10.1002/btpr.2019 · Source: PubMed

Acetone–Butanol–Ethanol Competitive Sorption Simulation from Single, Binary, and Ternary Systems in a Fixed-Bed of KA-I Resin

Jinglan Wu, Wei Zhuang, and Hanjie Ying
State Key Laboratory of Materials-Oriented Chemical Engineering, Nanjing 210009, P. R. China

College of Biotechnology and Pharmaceutical Engineering, Nanjing Tech University, Nanjing 210009, P. R. China

National Engineering Technique Research Center for Biotechnology, Nanjing 211816, P. R. China

Pengfei Jiao, Renjie Li, Qingshi Wen, Lili Wang, Jingwei Zhou, and Pengpeng Yang
College of Biotechnology and Pharmaceutical Engineering, Nanjing Tech University, Nanjing 210009, P. R. China

National Engineering Technique Research Center for Biotechnology, Nanjing 211816, P. R. China

DOI 10.1002/btpr.2019
Published online November 24, 2014 in Wiley Online Library (wileyonlinelibrary.com)

Separation of butanol based on sorption methodology from acetone–butanol–ethanol (ABE) fermentation broth has advantages in terms of biocompatibility and stability, as well as economy, and therefore gains much attention. In this work a chromatographic column model based on the solid film linear driving force approach and the competitive Langmuir isotherm equations was used to predict the competitive sorption behaviors of ABE single, binary, and ternary mixture. It was observed that the outlet concentration of weaker retained components exceeded the inlet concentration, which is an evidence of competitive adsorption. Butanol, the strongest retained component, could replace ethanol almost completely and also most of acetone. In the end of this work, the proposed model was validated by comparison of the experimental and predicted ABE ternary breakthrough curves using the real ABE fermentation broth as a feed solution. © 2014 American Institute of Chemical Engineers *Biotechnol. Prog.*, 31:124–134, 2015
Keywords: butanol, acetone, ethanol, modeling, competitive sorption

Introduction

Increased demand for energy, oil prices, predicted shortages of fossil fuels, and global warming have made the quest for alternative fuels a high priority.[1–3] One such alternative, biobutanol is a nonpetroleum-based, biodegradable and nontoxic fuel. It has several superior properties compared with bioethanol, including higher energy content, a lower hygroscopicity and volatility, a better blending ability with gasoline, and directly used in the conventional combustion engines without modification. Use of biobutanol as an alternative fuel is of great significance since it can help reduce the dependency on fossil fuels, lower environmental pollution, and promote grain transformation.[4–6]

Various in situ product isolation techniques have been investigated and applied to remove biobutanol from acetone–butanol–ethanol (ABE) fermentation broth, such as pervaporation, extraction, gas stripping, ionic liquids and vacuum.[7–16] Since these techniques are either inefficient or expensive when butanol exists in low concentrations, adsorption has received nowadays considerable attention,[17,18] in which the suitable sorbent plays an essential role. Wiehn et al.[18] used a commercially available Dowex Optipore L-493, a kind of hydrophobic polymer resin, to recover butanol from the fermentation broth. A greater than twofold improvement in butanol and total solvent production was achieved via this resin. In our previous work, a tailor-made weak-polar KA-I resin was demonstrated to adsorb butanol effectively and had a high affinity for butanol.[19] The adsorption equilibrium and kinetics of butanol on the KA-I resin was experimentally determined and simulated.[20] Furthermore, the effects of various operating conditions in terms of inlet flow rate, initial butanol concentration, and bed height on the sorption of butanol from aqueous solution on KA-I resin were investigated systematically. The Thomas, Yoon-Nelson, and Adams-Bohart models were successfully applied to describe experimental data obtained from the dynamic studies performed in the fixed-bed column to simulate the breakthrough curves and to determine the corresponding column kinetic constants.[21]

However, all the above-mentioned studies have been mainly focused on the sorption behaviors of pure butanol. As a matter of fact, besides butanol, there are two main impurities existing in the butanol fermentation broth, i.e., acetone and ethanol. It is recognized that in the multicomponent system, the adsorption capacity of each solute at equilibrium relies on the concentration of other components present locally. Depending on the composition of the real

Jinglan Wu and Pengfei Jiao contributed equally to this work.

Correspondence concerning the article should be addressed to H. Ying at yinghanjie@njtech.edu.cn).

fermentation broth, the competitive effects may significantly reduce the efficiency of the removal process. Moreover, as is well known, most of adsorption operations are carried out in the fixed-bed columns since the column system offers optimum conditions for enhancing the driving force (due to concentration gradient), which, in turn, improves sorption efficiency and mass transfer performance.[22] The design, operation, and optimization of sorption process in fixed-bed columns can be more easily accomplished by use of mathematical models which can predict the behavior of breakthrough curves under various operating conditions. Sulaymon and Ahmed[23] have established a general rate model (GRM) to describe the multicomponent competitive adsorption of furfural and phenolic compounds in a fixed bed column with activated carbon. This model is the most complicated one, which considers axial dispersion, film mass transfer, and pore diffusion resistance. Another chromatographic model, based on the solid linear driving force approach (so-called LDF model), has been often used to predict the competitive adsorption of organic compounds from aqueous phases as well. In LDF model, the film mass transfer and pore diffusion resistance are lumped into an effective mass transfer coefficient k_{eff}. This model is relatively simple and requires short computation time in comparison with the GRM.[24] Luz et al.[25] used this model to predict the breakthrough curves of binary synthetic sugar solutions successfully. More recently, this model was also applied to describe the competitive adsorption behaviors of quaternary mixture in the bioethanol fermentation system.[26]

However, to the best of our knowledge, the competitive sorption behaviors of ABE multiple fermentation broth components have not been described before. Since butanol, acetone, and ethanol are the main products presented in the broth, as a preliminary work, the LDF model is selected to simulate the acetone, butanol, and ethanol single breakthrough curves, and acetone–butanol, acetone–ethanol, and butanol–ethanol binary, as well as the acetone–butanol–ethanol ternary mixture competitive breakthrough curves. By comparison of the model predictions with the experimental data, the feasibility of the selected model can be then verified.

Materials and Methods

Solutions and resin

Analytical reagent grade acetone (C_3H_6O, molecular weight 58.08), butanol (C_4H_9OH, molecular weight 74.12), and ethanol (C_2H_6O, molecular weight 46.07), and other chemicals used in the fermentation were obtained from Sinopharm Chemical Reagent Co., Ltd and used without further purification. All solutions used in this study were prepared by measuring and dissolving the required amounts of solutes in deionized water.

The ABE fermentation broth was produced by fermentation of glucose using *Clostridium acetobutylicum* B3 (CGMCC No. 5234) as the bacterial strain, which was previously isolated from soil and was selected after UV mutagenesis.[27] The batch fermentation was conducted anaerobically in a 5 L serum bottle. The volume of the ABE production medium was 1.5 L, including 60 g/L glucose, 0.5 g/L K_2HPO_4, 0.5 g/L KH_2PO_4, 2.2 g/L CH_3COONH_4, 0.2 g/L $MgSO_4{\cdot}7H_2O$, 0.01 g/L $MnSO_4{\cdot}H_2O$, 0.01 g/L NaCl, 0.01 g/L $FeSO_4{\cdot}7H_2O$, 1 mg/L *p*-aminobenzoic acid, 1 mg/L thiamine, and 0.01 mg/L biotin. The fermentation broth was filtered by an ultrafiltration membrane unit (UOF4, Tianjin MOTIMO Membrane Technology Co., Ltd., Tianjin, China) to remove the microbial cells before it was used in the experiments.

Table 1. Physicochemical Properties of KA-I Resin

Matrix Structure	Polystyrene
Polarity	Polar
Particle size (mm)	0.8
Porosity (%)	65
Wet density (g/cm^3)	1.05
Surface area (m^2/g)	850–950
Average pore diameter (Å)	145–155
Pore volume (cm^3/g)	0.62–0.66
Skeletal density (g/cm^{-3})	0.70

The macroporous adsorption resin, KA-I, with a cross-linked polystyrene framework was obtained from the National Engineering Technique Research Center for Biotechnology (Nanjing, China). The physical properties of the resin have been shown in our previous work,[19] and also listed in Table 1.

Analytical procedures

The concentrations of solutes in the various sample solutions were determined by GC (Agilent 7890, Santa Clara, CA) equipped with a flame ionization detector (FID). The sample solutions were directly injected (1 μL) into a capillary column, Agilent HP-INNOWAX 19091N-236 (60 m $\times$ 0.25 mm $\times$ 0.25 μm, Agilent Technologies). The oven temperature was programmed as follows: the column held initially at 70°C for 0.5 min after injection, then increased to 190°C with 20°C/min. The temperatures of the injector and detector were set at 180 and 220°C, respectively. The carrier gas (nitrogen) was controlled at a flow rate of 2.0 mL/min and the split ratio was 1:90. Chromatographic data were recorded and integrated using Agilent data analysis software. Iso-butanol was added to the samples as the internal standard.[28]

Experimental methods

Static Equilibrium Adsorption Experiments. Batch uptake experiments were performed to study the single/ multicomponent equilibrium adsorption isotherms of butanol (or other solutes of interest) from single/multicomponent systems onto resins at the temperature of 298 K. The mass ratio of acetone: butanol: ethanol in ternary mixture solution was equal to 3:6:1, which was close to the ratio of these components in the actual final fermentation broth.[27] The solutions (50 mL) with one or more kinds of these three organic solvents were added to Erlenmeyer flasks (100 mL) containing 2 g wet resin. After that, the flasks were sealed and shaken at 120 rpm in a shaker for 8 h at 298 K to attain the equilibrium. Then a sample was withdrawn from the supernatant fluid with a syringe and the concentration of solute of interest was measured by GC. The equilibrium adsorption capacity (q_e) of the individual solute i on the resin was determined by the following relationship:

$$q_{i,e} = \frac{(c_{i,0} - c_{i,e})V}{m} \tag{1}$$

where $c_{i,0}$ and $c_{i,e}$ represents the initial and equilibrium aqueous concentration of butanol (or other solutes of interest), V is the volume of the solution, and m is the mass of the used resin.

Adsorption Kinetics Experiments. In order to better understand the interaction between butanol and ethanol adsorption on the resin, adsorption kinetics of butanol and ethanol in the single and binary systems were conducted in a constant temperature of 298 K with agitation at 120 rpm. The wet resin KA-I (15 g) was mixed with 375 mL of butanol or ethanol single aqueous solution or binary mixture solution. The concentration of butanol and ethanol was set 12 g/L and 2 g/L, respectively (approximately the same concentration as in the ABE fermentation broth). Samples about 0.5 mL were taken at predetermined time internals for the analysis of butanol and ethanol. Adsorption capacity at time t was calculated by the following equation:

$$q_t = \frac{(c_0 - c_t)V}{m} \tag{2}$$

where c_0 and c_t are the initial adsorbate concentration and concentration at time t, respectively.

Dynamic Column Adsorption Experiments. The experiments were conducted in glass columns of 20 cm length and 3.0 cm inner diameter, which allow for packing about 100 g of the KA-I resin. The fixed-bed operation was performed isothermally at 298 ± 1 K and the feed stream (influent) containing a desired initial amount of one or more components (acetone, butanol and ethanol as well as the ABE fermentation broth) was pumped into the column in a downflow mode. The flow rate was fixed at 5 mL/min, which was controlled by a constant flow peristaltic pump (BT00-300M, Hebei, China). Samples were collected at the outlet of the column (effluent) at pre-determined time intervals and the concentration of raffinate was periodically analyzed by GC.

All the experiments in this study were carried out at least three times to ensure reproducibility and the reported values were the average of three data sets.

Model calculation

Adsorption Equilibrium. In the single-component system, the experimental equilibrium data of each individual solute obtained was fitted by the Langmuir isotherm model which is represented as follows:

$$q_{i,e} = \frac{q_{i,m}K_i c_{i,e}}{1 + K_i c_{i,e}} = \frac{a_i c_{i,e}}{1 + b_i c_{i,e}} \tag{3}$$

In the multicomponent systems, the competitive Langmuir isotherm model was used to describe the adsorption equilibrium of each solute:[29]

$$q_{i,e} = \frac{q_{i,m}K_i c_{i,e}}{1 + \sum_j^N K_j c_{j,e}} = \frac{a_i c_{i,e}}{1 + \sum_j^N b_j c_{j,e}} \tag{4}$$

where $q_{i,m}$ is the Langmuir isotherm constant, $c_{i,e}$ represents the equilibrium concentration of species i, and K_i is equilibrium coefficient, a_i is the product of the Langmuir isotherm constant which equals to the product of $q_{i,m}$ and K_i, b_i is equal to the Langmuir isotherm constant K_i, N is the number of components in the system. The model parameters, i.e., a_i and b_i were obtained with the commercial software gPROMS V 3.1.4 (Parameter Estimations Section).[30]

Fixed-Bed Column Model. The LDF model is used in this work to simulate the sorption behaviors of the specific component in the fixed bed due to its simplicity. The model comprises a mass balance equation, adsorption isotherm, and a linear rate equation. The assumptions of this model are as follows: (1) fluid density and viscosity are constant; (2) isothermal operation; (3) radial distributions are negligible; (4) Constant fluid flow rate; (5) angular variation is neglected; (6) mass transfer rate in the adsorption process is described by linear driving force rate equation. The differential mass balance in a volume element for species i in the liquid phase can be expressed:[31]

$$v\frac{\partial c_i}{\partial z} + \frac{\partial c_i}{\partial t} + \rho\frac{1-\varepsilon_b}{\varepsilon_b}\frac{\partial q_i}{\partial t} = D_L\frac{\partial^2 c_i}{\partial z^2} \tag{5}$$

The mass transfer rate is represented by a linear driving force (LDF) equation according to Glueckauf:[32]

$$\frac{\partial q_i}{\partial t} = k_{eff}(q_{i,e} - q_i) \tag{6}$$

where v is the interstitial velocity, equal to $Q_f/(A\cdot\varepsilon_b)$, A is the cross sectional area of column, Q_f is the volumetric flow rate, z is the axial position, t is the time, ρ and ε_b are the density of adsorbent and bed porosity which was obtained by the determination of void volume corresponding to the volume of the deionized water needed to brim the bed,[22] D_L is the axial dispersion coefficient, and k_{eff} is the effective mass transfer coefficient. The following empirical correlation was used to calculate D_L:[33]

$$D_L = 0.44D_m + 0.83Ud_p \tag{7}$$

where d_p is the particle diameter, U is the superficial velocity, D_m is the molecular coefficient and could be calculated by the Wilke–Chang equation:[34]

$$D_m = \frac{7.4\times10^{-8}(\varphi M_B)^{1/2}T}{\eta_B V_A^{0.6}} \tag{8}$$

in which φ is association parameter, M_B is the molecular weight of water, T is operating temperature, η_B is the viscosity of solution, and V_A is the molar volume of adsorbate at normal boiling point.

The boundary conditions are written as was suggested by Danckwerts:[35]

$$z = 0, D_L\frac{\partial c_i}{\partial z}\Big|_{z=0} = v(c_i\Big|_{z=0} - c_{0,i}) \tag{9}$$

$$z = L, \frac{\partial c_i}{\partial z}\Big|_{z=L} = 0 \tag{10}$$

Initial conditions are:

$$t = 0, \quad q_i = 0 \quad c_i = 0. \tag{11}$$

Adsorption equilibrium isotherm of species i in single/multicomponent systems can be described by the Langmuir isotherm Eq. 3 or the competitive Langmuir isotherm models Eq. 4.

This mathematical model was solved by the commercial software MATLAB 2010a. The axial domain was discretized using orthogonal collocation on finite elements method. Twenty finite elements in the discretization was used in order to satisfy the global mass balance relative error (<0.1%). After the discretization step, the time integration is performed by the ordinary differential equation solver ODE23 in MATLAB 2010a. Absolute and relative tolerance 10^{-5} were used. The effective mass transfer coefficient k_{eff}

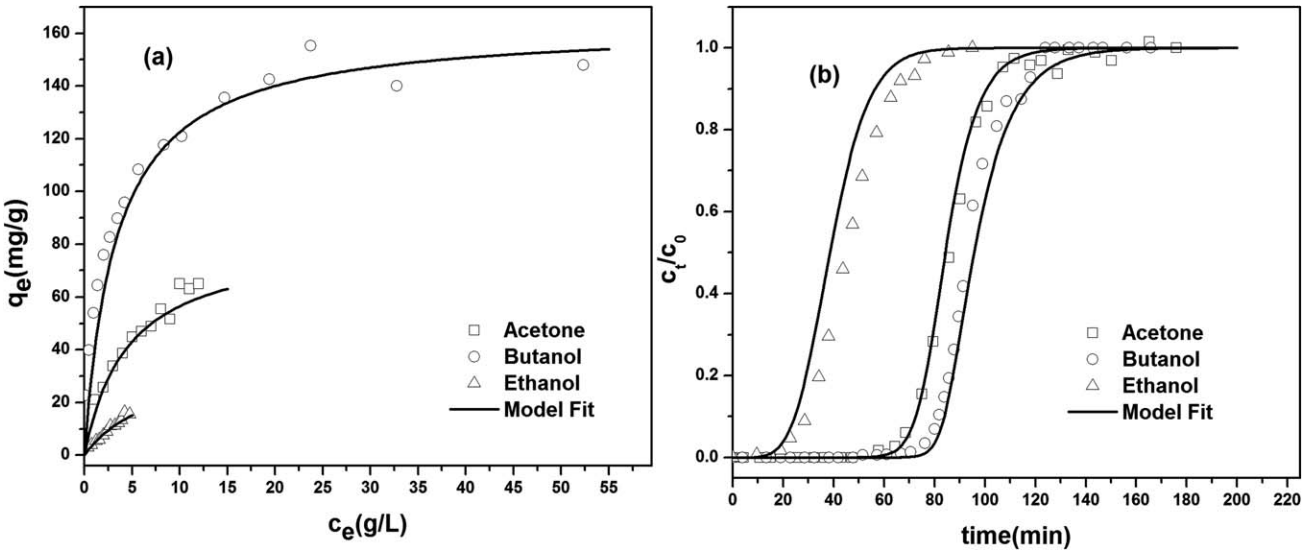

Figure 1. (a) Adsorption isotherms of acetone, butanol and ethanol onto KA-I resin in single component system at the temperature of 298 K; (b) Breakthrough curves of acetone, butanol, and ethanol in single component system.

was determined by minimizing the objective function given as follows:

$$F(p)=\sum_{i}^{n}\sum_{j}^{N}\left(\frac{c_{i,pre}(t_j)-c_{i,out}(t_j)}{c_{i,out}(t_j)}\right)^2 \quad (12)$$

where n is the number of solutes and N is the number of experimental data, $c_{i,\mathrm{pre}}$ is the concentration in the outlet flow at time t_j calculated by the model and $c_{i,\mathrm{out}}$ is the experimental concentration at time t_j.

Results and Discussion

Modeling of the sorption behaviors of ABE single system

The single-component adsorption equilibrium isotherms of acetone, butanol, and ethanol aqueous solutions on the KA-I resin at 298 K, along with the prediction curves calculated by the corresponding Langmuir isotherm model are shown in Figure 1a. The prediction results fit the experimental data fairly well. The Langmuir model parameters in terms of a and b for the individual components are given in Table 2. It is clear that the relative adsorption affinity of three compounds to the resin follows the order: butanol > acetone > ethanol. The saturation capacities of acetone and ethanol, two main impurities existing in the real fermentation broth, were much smaller than that of butanol. This can be explained by the polarities of the components. According to the mechanism of hydrophobic interaction between the sorbate and the resin, there would be a decrease in affinity to resin with an increase in polarity from the sorbate, that is, from butanol to acetone to ethanol.[36]

The breakthrough curves of each single component were obtained by frontal analysis method on the preparative column packed with KA-I resin. For the sake of comparison, the breakthrough curve was represented as the effluent/influent concentration ratio (c/c_0) versus time. Figure 1b shows the experimental and the simulated concentration histories for acetone, butanol and ethanol in the single-component system at 298 K. The values of objective function $F(p)$ given in Table 3 are all lower than 5.78 indicating the model can be used to predict the acetone, butanol and ethanol adsorption behaviors on the resin. Since the adsorption affinities of ethanol and acetone to the resin are weak, the packed bed is soon saturated with these solutes, whereas butanol shows the strongest adsorption affinity to the resin, which is consistent

Table 2. Isotherm Parameters for Solutes Adsorption on Resin KA-I

	Solute	a (mL/g)	b (L/g)
Single-component system	Acetone	18.2 ± 0.1	$0.22 \pm 5.0 \times 10^{-3}$
	Butanol	49.0 ± 0.2	$0.30 \pm 7.5 \times 10^{-3}$
	Ethanol	5.0 ± 0.1	$0.13 \pm 3.1 \times 10^{-3}$
Binary-component system	Acetone	14.0 ± 0.1	$0.16 \pm 4.0 \times 10^{-3}$
	Butanol	51.5 ± 0.3	$0.25 \pm 8.0 \times 10^{-3}$
	Acetone	18.9 ± 0.2	$0.20 \pm 6.7 \times 10^{-3}$
	Ethanol	6.1 ± 0.2	$0.10 \pm 2.8 \times 10^{-3}$
	Butanol	51.5 ± 0.2	$0.25 \pm 5.4 \times 10^{-3}$
	Ethanol	4.3 ± 0.1	$0.09 \pm 6.1 \times 10^{-3}$
Ternary-component system	Acetone	14.5 ± 0.1	$0.15 \pm 4.3 \times 10^{-3}$
	Butanol	48.0 ± 0.2	$0.30 \pm 6.0 \times 10^{-3}$
	Ethanol	3.6 ± 0.1	$0.05 \pm 5.2 \times 10^{-3}$
Ternary-component system*	Acetone	14.5	0.15
	Butanol	48.0	0.30
	Ethanol	3.6	0.05

*Adsorption of ABE from actual fermentation broth.

Table 3. Dynamic Parameters of ABE Single, Binary, and Ternary Adsorption Systems

	Solute	c_0 (g/L)	k_{eff} (min^{-1})	D_L ($\times 10^{-2}$ cm^2/min)	$F(p)$
Single-component system	Acetone	6.0	0.20 ± 0.015	4.68	0.93 ± 0.07
	Butanol	12.0	0.10 ± 0.010	4.67	5.78 ± 0.21
	Ethanol	2.0	0.30 ± 0.009	4.68	3.76 ± 0.11
Binary-component system	Acetone	6.0	0.25 ± 0.017	4.68	3.31 ± 0.54
	Butanol	12.0	0.10 ± 0.008	4.67	
	Acetone	6.0	0.20 ± 0.011	4.68	8.12 ± 0.32
	Ethanol	2.0	0.31 ± 0.010	4.68	
	Butanol	12.0	0.10 ± 0.007	4.67	6.28 ± 0.24
	Ethanol	2.0	0.33 ± 0.015	4.68	
Ternary-component system	Acetone	6.0	0.25 ± 0.012	4.68	6.15 ± 0.13
	Butanol	12.0	0.12 ± 0.016	4.67	
	Ethanol	2.0	0.27 ± 0.004	4.68	
Ternary-component system*	Acetone	6.18	0.23 ± 0.020	4.68	15.90 ± 1.04
	Butanol	10.48	0.12 ± 0.010	4.67	
	Ethanol	1.20	0.28 ± 0.020	4.68	

*Adsorption of ABE from actual fermentation broth.

with the results obtained from the equilibrium data (Figure 1a).

The effective mass transfer coefficient k_{eff} was obtained by the best fitting procedure of the sets of breakthrough data in which the objective function $F(p)$ has been minimized (Eq. 12). The k_{eff} of these three solutes on the KA-I resin is quite fast as one can conclude from the estimated values of the k_{eff}. The axial dispersion coefficient D_L are almost identical for the ABE ternary component ($\sim 4.67 \times 10^{-2}$ cm^2/min, see Table 3), which is approximate 100 times greater than the molecular diffusion coefficient D_m (7.65, 6.25, and 8.74 $\times 10^{-4}$ cm^2/min for ABE, respectively). According to Eq. 7, the first term on the right hand equation represents the molecular diffusion in the interparticle voids, and the second term is the eddy diffusion. Both of them contribute to the axial dispersion. The effect of eddy diffusion becomes significant at high flow rate. Therefore, the values of D_L are much greater than the molecular diffusion coefficient. The same order of magnitude of D_L has been reported by Zhou et al.[26] in the adsorption of ethanol and Qian et al.[37] in the adsorption of cAMP as well.

Modeling of the sorption behaviors of ABE binary and ternary systems

The competitive adsorption isotherms of ABE binary and ternary mixtures are showed in Figure 2, in which the points represent experimental data and the lines are the competitive Langmuir model simulations. Good agreement between the experimental data and the model predictions can be seen. For the sake of comparison, the adsorption isotherms of ABE single-component are presented in Figure 2 as well. It can be observed the uptake of strong adsorbed component in the binary systems is nearly the same as in the single system. Due to the competitive effect, the uptake of weak adsorbed component is reduced greatly compared with its pure component. However, it is interesting to see in the binary butanol-ethanol (BE) system (Figure 2a), the uptake of weak adsorbed component, ethanol is reduced significantly, whereas the uptake of strong adsorbed component, butanol is slightly increased. It seems the butanol adsorption is enhanced in the presence of ethanol.

In order to better understand the interaction between butanol and ethanol in the BE binary adsorption system, kinetics studies were conducted to investigate the competitive adsorption performances of these two components on the resin. The concentration decay curves of butanol and ethanol in binary system are presented in Figure 3. It can be observed the concentration of ethanol decreased firstly and then increased, indicating the ethanol molecules were initially adsorbed on the resin and subsequently replaced by butanol. The competitive effects existed in the BE adsorption system.

The relative adsorption of ethanol ($(A_r)_E$) and butanol ($(A_r)_B$) as well as the adsorption selectivity (S) in the BE binary system were calculated according to the following equations:[38]

$$A_r = \frac{q_{t,B}}{q_{t,S}} \tag{13}$$

$$S = \frac{(A_r)_B}{(A_r)_E} \tag{14}$$

where $q_{t,B}$ and $q_{t,S}$ are the amount of adsorption of specific adsorbate in the binary system and single system at time t respectively.

The relative adsorption and adsorption selectivity were presented in Figure 4. As can be seen, the $(A_r)_E$ were low during the adsorption (~ 0.5), indicating adsorption of ethanol in the binary adsorption system was inhibited by the presence of butanol. Meanwhile, the $(A_r)_B$ were exhibited a high ratio (>1). Butanol was excessive in our binary adsorption system. The S values showed an increasing trend which suggested the adsorption favor to the butanol molecules.

Thompson et al.[39] investigated the adsorption mechanisms of single component ABE on the immobilized calixarene cavities. They pointed out that ethanol and butanol were inclined to insert their alkyl chains into the calixarene cavities to form inclusion complexes, whereas their hydroxyl groups interacted with solvent water via hydrogen bonding. The complexes were controlled by van der Waals interactions. In our BE binary adsorption system, the van der Waals interactions, i.e., hydrophobic interactions played an important role in adsorption. The hydrophobic interaction between ethanol and the resin was weaker than that of butanol with the resin. Moreover, the infinite-dilution activity coefficient of butanol in water at 298 K is 51.2,[40] much higher than that of ethanol in water (3.91).[41] Consequently, butanol has stronger affinity to resin than ethanol, resulting in the reduction of ethanol adsorption capacity in the BE binary system.

The $(A_r)_B$ values were a little more than unit indicating the adsorption capacity of butanol was enhanced slightly in the BE binary system. Do and Do[42] investigated the binary mixture adsorption of ethylene, ethane, nitrogen, and argon

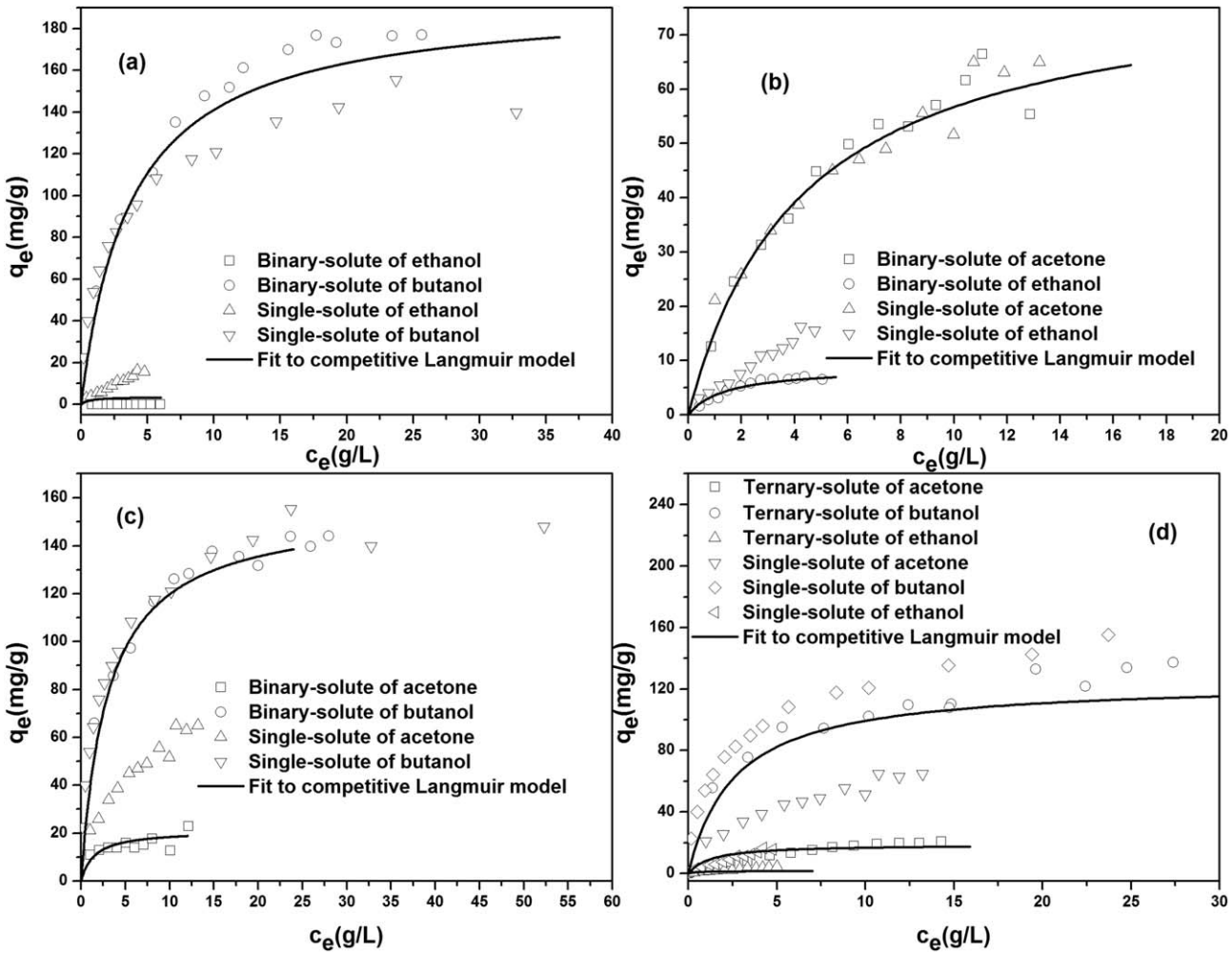

Figure 2. (a–c) Adsorption isotherms of butanol and ethanol (a), acetone and ethanol (b), acetone and butanol (c) onto KA-I resin in binary component system at the temperature of 298 K; (d) adsorption isotherms of acetone, butanol and ethanol onto KA-I resin in ternary component system at the temperature of 298 K.

on graphitized thermal carbon black. They observed in the presence of another adsorbate, i.e., ethane, nitrogen, and argon, the adsorbed amount of ethylene was enhanced at low pressure. They explained that the enhancement in the ethylene adsorption was due to the lateral interaction between adsorbate molecules. They called such an enhancement in adsorption the co-operative adsorption and pointed out the co-operation was possible for practically all mixtures as long as the sorbent surface was only fractionally covered. Zhang

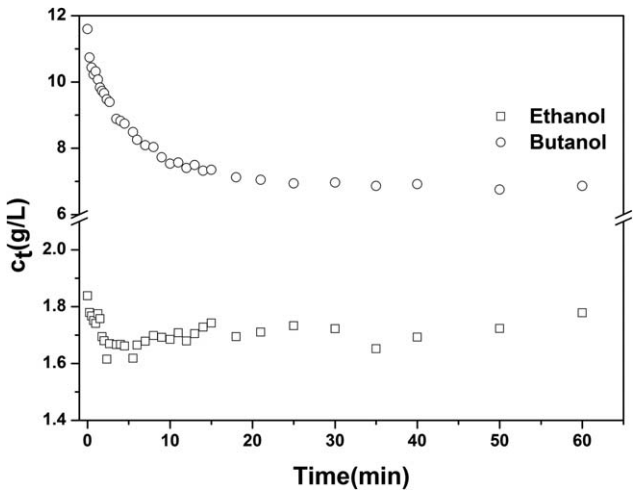

Figure 3. Adsorption kinetics curves of butanol and ethanol in binary system.

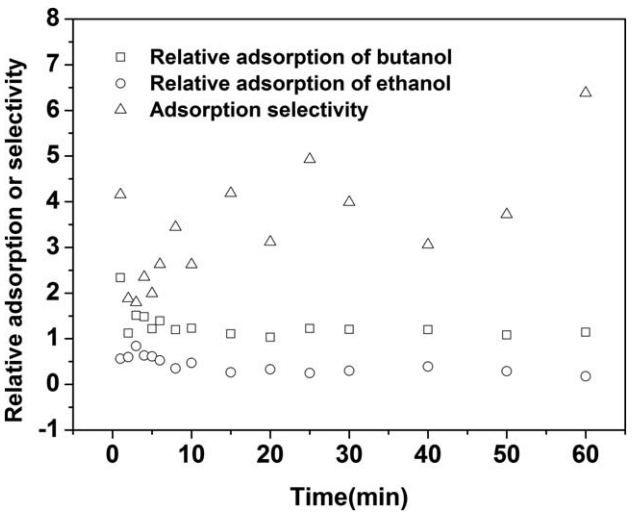

Figure 4. Relative adsorption and adsorption selectivity of butanol and ethanol in binary system.

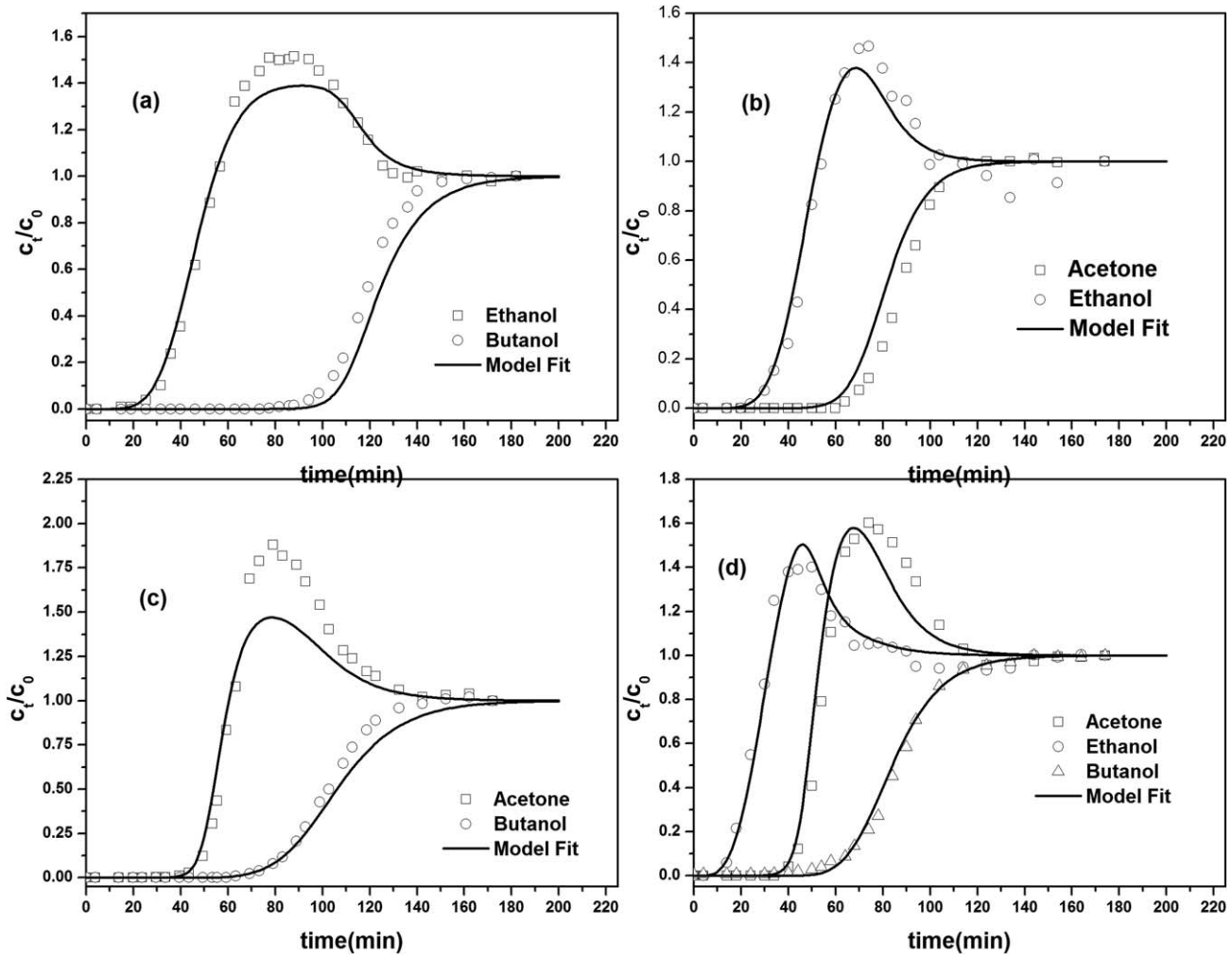

Figure 5. (a–c) Breakthrough curves of butanol and ethanol (a), acetone and ethanol (b), acetone and butanol (c) onto KA-I resin in binary component system at the temperature of 298 K; (d) breakthrough curves of acetone, butanol and ethanol onto KA-I resin in ternary component system at the temperature of 298 K.

et al.[43] investigated the adsorption behaviors of phenol and aniline on nonpolar macroreticular adsorbents. They observed at the high equilibrium concentrations, the total uptake amounts of phenol and aniline in binary-component systems were larger than that in single-component systems. The cooperative adsorption effects resulting from the hydrogen bonding or weak acid-base interaction between phenol and aniline were proposed as well. Teng et al.[44] studied the interaction between congo red and copper in a binary adsorption system. Adsorption capacity for congo red decreased in the presence of Cu(II) while it increased slightly for Cu(II). The enhanced adsorption phenomenon was explained by that a congo red–copper complex was formed and Cu(II) attached to the adsorbent individually or was bound by the congo red-copper complex, which resulted in an increase adsorption capacity of Cu(II) in the binary mixture. Klimaszewski et al.[45] investigated the intermolecular interaction between ethanol and butanol by experimental determination of the relative static permittivity with different mole ratio of ethanol and butanol mixtures. The results show the ability of ethanol-butanol molecules to create intermolecular associates through hydrogen bonds is stronger than butanol-butanol molecules. In our BE binary adsorption system, although most of ethanol were replaced by butanol, a few of the ethanol molecules still remained on the resin, providing active sites to bond butanol via hydrogen bonds. This might be the reason for the slightly enhanced adsorption of butanol in the BE binary system. However, the interaction between adsorbates can be rather complicated. In literature, the spectroscopy analysis, i.e., FTIR and XPS, was commonly used to elucidate the interaction mechanisms.[44] To clarify the interactions, these analysis methods or even the molecular simulation could be used, which will be considered in our future work.

The competitive breakthrough curves of the ABE binary and ternary components are presented in Figure 5, together with the model calculations. Good agreement between the experimental data and the model predictions can be seen (the values of objective function $F(p)$ are all lower than 8.12 in Table 3). It indicates the LDF model incorporated with the competitive isotherm models are correct. The outlet concentrations of the weaker retained component exceed the inlet concentration ($c/c_0 > 1$), which is due to the displacement by the stronger adsorbed component. This is a typical characteristic of the competitive adsorption.[29,46] In our case, the adsorbed ethanol (the most weakly retained substance) is displaced by acetone (middle weakly retained substance) in Figure 5b, whereas the adsorbed acetone is displaced by butanol (the most strongly retained substance) in Figure 5c. Butanol exhibits the highest affinity to the adsorbent and is thus not overshoot by any other compound.

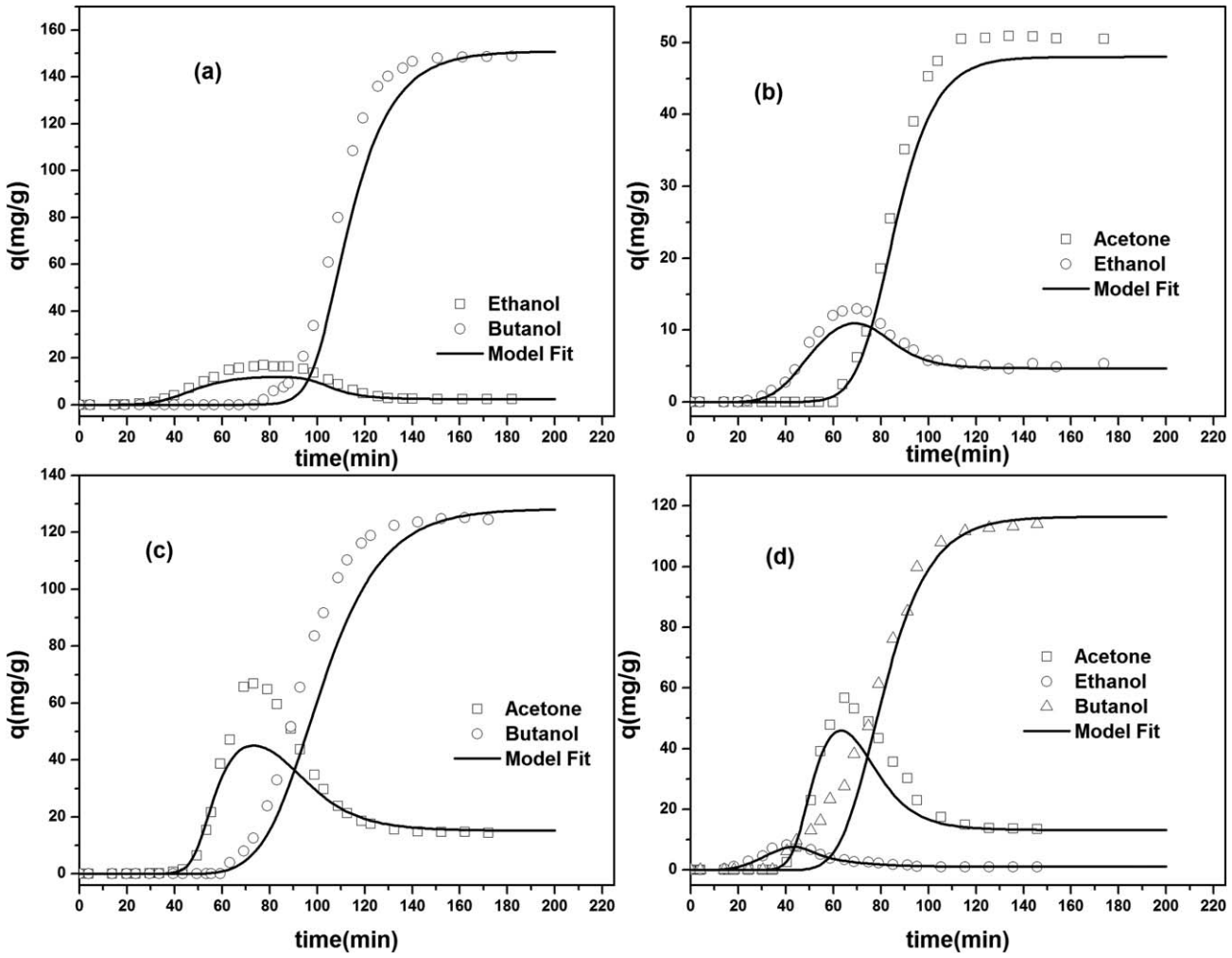

Figure 6. (a–c) Sorption of butanol and ethanol (a), acetone and ethanol (b), acetone and butanol (c) onto KA-I resin at the outlet of the column in binary component system at the temperature of 298 K; (d) sorption of acetone, butanol, and ethanol onto KA-I resin at the outlet of the column in ternary component system at the temperature of 298 K.

From Table 3, it can be observed that the effective mass transfer coefficient k_{eff} in the binary and ternary adsorption systems are almost identical to that of single adsorption systems. The phenomenon can be explained by that the effective mass transfer coefficient is relevant to internal and external mass transfer resistance, and the internal and external mass transfer coefficient of one solute are almost independent of the existence of other component at lower concentration.[23,47] Silva et al.[48] has predicted the breakthrough curves of Cr(III) ion and Cu(II) ion in binary component system successfully with the values of effective mass transfer coefficient from the single component system.

The ABE binary and ternary mixtures sorption on KA-I resin as a function of time is depicted in Figure 6. As seen in the figure, the model describes the evolution of the adsorbed component very well. There are overshoots observed for the weakly adsorbed component which are related to the overshoots exhibited in Figure 5. When the overshoot of the weakly adsorbed component occurs, the continuous tendency of this component to get accumulated on the sorbent is broken reaching a maximum accumulation. From this point the concentration of this component on the solid phase progressively decreases until it reaches a constant accumulation value. The final constant accumulation values of ethanol, acetone and butanol in ABE ternary system are 0.1, 18, and 112.8 mg/g, respectively (see Figure 6d), which correspond to the values obtained from the ternary competitive equilibrium isotherm (see Figure 2d).

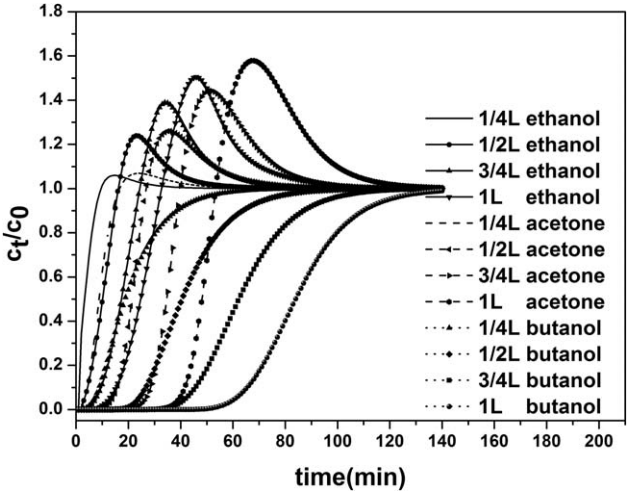

Figure 7. Breakthrough curves of acetone, butanol and ethanol at various fixed bed positions (1/4 L, 1/2 L, 3/4 L, 1 L) in ternary component system at the temperature of 298 K.

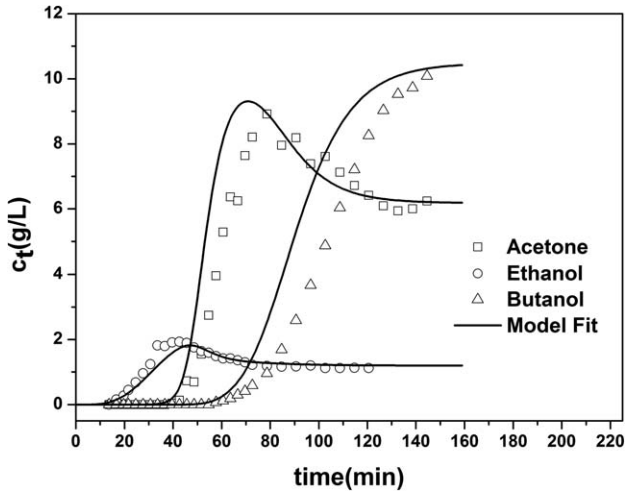

Figure 8. Breakthrough curves of acetone, butanol, and ethanol from actual fermentation broth.

For a better understanding of the competitive adsorption process, Figure 7 schematically shows the development of the ABE mixtures breakthrough curves at various column positions. In Figure 7 (the ABE ternary mixture system), it can be observed ethanol, acetone and butanol are absorbed by the KA-I resin initially. However, due to the difference in the propagation velocities[22] of moving fronts for the competitor species, the less favorable species ethanol propagates with the faster moving front whereas acetone and butanol (more favorably adsorbed components) are preferentially retained in the region of column inlet. As this region is saturated with acetone (the second favorable species), this species trickles along the column so that most of ethanol that is initially adsorbed is displaced and released to the solution resulting in the outlet concentrations higher than the concentrations of the feed solution. This behavior characterizes the competitive adsorption. Since butanol is the most favorably adsorbed species, its propagation velocity of moving fronts is the lowest. With the course of adsorption process, it displaces the adsorbed acetone. When acetone and butanol break through, displacement is reduced, and the concentrations of ABE tend towards their inlet values.

Column dynamic adsorption process with actual ABE fermentation broth

The column experiment was performed with the real ABE fermentation broth used as a feed solution. The concentrations of ABE in the fermentation broth were 6.18 g/L, 10.48 g/L, and 1.2 g/L, respectively. The Langmuir isotherm constants (a_i and b_i) from ABE ternary-component isotherm were used in the real fermentation broth prediction. The axial dispersion coefficient D_L and the effective mass transfer coefficient k_{eff} were given in Table 3. The experimental ABE breakthrough curves were shown in Figure 8. Meanwhile, the LDF model prediction was presented in Figure 8 as well. The value $F(p)$ was 15.90. The results showed that the model could provide a general description to the breakthrough curve of ABE from the fermentation broth. The LDF model therefore can be validated.

Conclusion

Computational and theoretical modeling has become an important tool for the characterization, development of packed beds. Relevant breakthrough curves would provide much valuable information for design of a fixed bed. In this article, the LDF model incorporated with the competitive Langmuir model was proposed to simulate the breakthrough curves of ABE single, binary and ternary mixtures. Butanol was the strongest retained component, acetone the middle while ethanol the weakest one. In ternary system, butanol could almost replace ethanol completely and also most of acetone, indicating the KA-I resin has a good adsorption selectivity toward butanol over acetone and ethanol.

Acknowledgment

The work was supported in part by the grand from the National Outstanding Youth Foundation of China (Grant No.: 21025625), 473000, 12KJB530003, and 21306086. The authors acknowledge the financial support provided by the National High-Tech Research and Development Plan of China (863 Program, 2012AA021202).

Notation

φ = association parameter
η_B = viscosity of solution (cp)
ε_b = void ratio of KA-I packed bed
A = cross-sectional area of column (cm^2)
A_r = relative adsorption
a = competitive Langmuir isotherm constant (mL/g)
b = competitive Langmuir isotherm constant (L/g)
c = liquid phase concentration (g/L)
c_0 = initial concentration of solute in solution (g/L)
c_e = equilibrium concentration of solute in solution (g/L)
c_{out} = concentration of solute at the effluent solution at time t_j (g/L)
c_{pre} = concentration at time t_j in the outlet flow calculated by the model (g/L)
d_p = particle diameter (cm)
D_m = molecular coefficient (cm^2/min)
D_L = axial dispersion coefficient (cm^2/min)
K = Langmiur isotherm constant (L/g)
k_{eff} = effective mass transfer coefficient (min^{-1})
M_B = molecular weight of H_2O
m = mass of the wet resin (g)
Q_f = inlet feed flow rate (mL/min)
q_i = adsorption capacities of adsorbate at t time (mg/g)
q_e = adsorption capacities of adsorbate at exhaustion time (mg/g)
q_m = maximum adsorption capacity (mg/g)
S = adsorption selectivity
T = temperature (K)
t = time (min)
U = superficial flow velocity (cm/min)
V = volume of the aqueous solution (L)
V_A = molal volume of solute at normal boiling point (mL/(g mol)
z = bed height (cm)

Literature Cited

1. Lin Y-L, Blaschek HP. Butanol production by a butanol-tolerant strain of *Clostridium acetobutylicum* in extruded corn broth. *Appl Environ Microbiol*. 1983;45:966–973.
2. Yan Y, Liao JC. Engineering metabolic systems for production of advanced fuels. *J Ind Microbiol Biotechnol*. 2009;36:471–479.

3. Jang YS, Malaviya A, Lee J, Im JA, Lee SY, Lee J, Eom MH, Cho JH, Seung DY. Metabolic engineering of *clostridium acetobutylicum* for the enhanced production of isopropanol-butanol-ethanol fuel mixture. *Biotechnol Prog*. 2013;29:1083–1088.
4. Gnansounou E, Dauriat A, Wyman C. Refining sweet sorghum to ethanol and sugar: economic trade-offs in the context of North China. *Bioresour Technol*. 2005;96:985–1002.
5. Lee D-H, Lee D-J. Biofuel economy and hydrogen competition. *Energy Fuel*. 2007;22:177–181.
6. Kim S, Dale BE. Life cycle assessment of fuel ethanol derived from corn grain via dry milling. *Bioresour Technol*. 2008;99: 5250–5260.
7. Ikegami T, Negishi H, Sakaki K. Selective separation of n-butanol from aqueous solutions by pervaporation using silicone rubber-coated silicalite membranes. *J Chem Technol Biotechnol*. 2011; 86: 845–851.
8. Maddox IS. The acetone-butanol-ethanol fermentation: recent progress in technology. *Biotechnol Genet Eng*. 1989;7: 189–220.
9. Groot W, Van Der Lans R, Luyben K. Technologies for butanol recovery integrated with fermentations. *Process Biochem*. 1992; 27:61–75.
10. Qureshi N, Maddox IS, Friedl A. Application of continuous substrate feeding to the ABE fermentation: relief of product inhibition using extraction, perstraction, stripping, and pervaporation. *Biotechnol prog*. 1992;8:382–390.
11. Vane LM. A review of pervaporation for product recovery from biomass fermentation processes. *J Chem Technol Biotechnol*. 2005;80:603–629.
12. Ezeji TC, Qureshi N, Blaschek HP. Production of acetone butanol (AB) from liquefied corn starch, a commercial substrate, using *Clostridium beijerinckii* coupled with product recovery by gas stripping. *J Ind Microbiol Biotechnol*. 2007;34:771–777.
13. Schügerl K. Integrated processing of biotechnology products. *Biotechnol Adv*. 2000;18:581–599.
14. Fadeev AG, Meagher MM. Opportunities for ionic liquids in recovery of biofuels. *Chem Commun*. 2001:295–296.
15. Wang Y, Chung TS, Wang H. Polyamide–imide membranes with surface immobilized cyclodextrin for butanol isomer separation via pervaporation. *AIChE J*. 2011;57:1470–1484.
16. Mariano AP, Qureshi N, Maciel Filho R, Ezeji TC. Assessment of in situ butanol recovery by vacuum during acetone butanol ethanol (ABE) fermentation. *J Chem Technol Biotechnol*. 2012; 87:334–340.
17. Oudshoorn A, Van Der Wielen LA, Straathof AJ. Assessment of options for selective 1-butanol recovery from aqueous solution. *Ind Eng Chem Res*. 2009;48:7325–7336.
18. Wiehn M, Staggs K, Wang Y, Nielsen DR. In situ butanol recovery from *Clostridium acetobutylicum* fermentations by expanded bed adsorption. *Biotechnol Prog*. 2014; 30:68–78.
19. Lin X, Wu J, Jin X, Fan J, Li R, Wen Q, Qian W, Liu D, Chen X, Chen Y, Xie J, Bai J, Ying H. Selective separation of biobutanol from acetone-butanol-ethanol fermentation broth by means of sorption methodology based on a novel macroporous resin. *Biotechnol Prog*. 2012;28:962–72.
20. Lin X, Wu J, Fan J, Qian W, Zhou X, Qian C, Jin X, Wang L, Bai J, Ying H. Adsorption of butanol from aqueous solution onto a new type of macroporous adsorption resin: Studies of adsorption isotherms and kinetics simulation. *J Chem Technol Biotechnol*. 2012;87:924–931.
21. Lin X, Li R, Wen Q, Wu J, Fan J, Jin X, Qian W, Liu D, Chen X, Chen Y, Xie J, Bai J, Ying H. Experimental and modeling studies on the sorption breakthrough behaviors of butanol from aqueous solution in a fixed-bed of KA-I resin. *Biotechnol Bioproc E*. 2013;18:223–233.
22. Kleinübing SJ, Guibal E, Da Silva EA, Da Silva MGC. Copper and nickel competitive biosorption simulation from single and binary systems by *Sargassum filipendula*. *Chem Eng J*. 2012; 184:16–22.
23. Sulaymon AH, Ahmed KW. Competitive adsorption of furfural and phenolic compounds onto activated carbon in fixed bed column. *Environ Sci Technol*. 2008;42:392–397.
24. Kaczmarski K, Antos D, Sajonz H, Sajonz P, Guiochon G. Comparative modeling of breakthrough curves of bovine serum albumin in anion exchange chromatography. *J Chromatogr A*. 2001;925:1–17.
25. Luz DA, Rodrigues AK, Silva FR, Torres AE, Cavalcante CL Jr, Brito ES, Azevedo DC. Adsorptive separation of fructose and glucose from an agroindustrial waste of cashew industry. *Bioresour Technol*. 2008;99:2455–2465.
26. Zhou J, Wu J, Liu Y, Zou F, Wu J, Li K, Chen Y, Xie J, Ying H. Modeling of breakthrough curves of single and quaternary mixtures of ethanol, glucose, glycerol and acetic acid adsorption onto a microporous hyper-cross-linked resin. *Bioresour Technol*. 2013;143:360–368.
27. Liu D, Chen Y, Li A, Ding F, Zhou T, He Y, Li B, Niu H, Lin X, Xie J, Chen X, Wu J, Ying H. Enhanced butanol production by modulation of electron flow in *Clostridium acetobutylicum* B3 immobilized by surface adsorption. *Bioresour Technol*. 2013;129:321–328.
28. Lin X, Fan J, Wen Q, Li R, Jin X, Wu J, Qian W, Liu D, Xie J, Bai J. Optimization and validation of a GC–FID method for the determination of acetone-butanol-ethanol fermentation products. *J Chromatogr Sci*. 2014;52:264–270.
29. Shirazi DG, Felinger A, Katti AM. *Fundamentals of Preparative and Nonlinear Chromatography*. Amsterdam: Academic Press; 2006.
30. Wu J, Peng Q, Arlt W, Minceva M. Model-based design of a pilot-scale simulated moving bed for purification of citric acid from fermentation broth. *J Chromatogr A*. 2009;1216:8793–8805.
31. Schmidt-Traub H. *Preparative Chromatography*. Weinheim: John Wiley & Sons; 2005.
32. Glueckauf E. Theory of chromatography. Part 10. Formulae for diffusion into spheres and their application to chromatography. *Trans Faraday Soc*. 1955;51:1540–1551.
33. Suzuki M, Smith JM. Axial dispersion in beds of small particles. *Chem Eng J*. 1972;3:256–264.
34. Wilke CR, Chang P. Correlation of diffusion coefficients in dilute solutions. *AIChE J*. 1955;1:264–270.
35. Danckwerts PV. Continuous flow systems: distribution of residence times. *Chem Eng Sci*. 1953;2:1–13.
36. Oudshoorn A, Van Der Wielen LA, Straathof AJ. Adsorption equilibria of bio-based butanol solutions using zeolite. *Biochem Eng J*. 2009;48:99–103.
37. Qian W, Wu J, Yang L, Lin X, Chen Y, Chen X, Xiong J, Bai J, Ying H. Computational simulations of breakthrough curves in cAMP adsorption processes in ion-exchange bed under hydrodynamic flow. *Chem Eng J*. 2012;197:424–434.
38. Wang S, Ariyanto E. Competitive adsorption of malachite green and Pb ions on natural zeolite. *J Colloid Interface Sci*. 2007; 314:25–31.
39. Thompson AB, Scholes RC, Notestein JM. Recovery of dilute aqueous acetone, butanol, and ethanol with immobilized calixarene cavities. *ACS Appl Mater Interfaces*. 2014;6:289–297.
40. Hovorka Š, Dohnal VR, Roux AH, Roux-Desgranges G. Determination of temperature dependence of limiting activity coefficients for a group of moderately hydrophobic organic solutes in water. *Fluid Phase Equilibr*. 2002;201:135–164.
41. Vrbka P, Fenclová D, Laštovka V, Dohnal V. Measurement of infinite dilution activity coefficients of 1-alkanols (C1–C5) in water as a function of temperature (273–373K). *Fluid Phase Equilibr*. 2005;237:123–129.
42. Do D, Do H. Cooperative and competitive adsorption of ethylene, ethane, nitrogen and argon on graphitized carbon black and in slit pores. *Adsorption*. 2005;11:35–50.
43. Zhang W-M, Chen J-L, Pan B-C, Zhang Q-X. Competitive and cooperative adsorption behaviors of phenol and aniline onto nonpolar macroreticular adsorbents. *J Environ Sci*. 2005;17: 529–534.
44. Teng S-X, Wang S-G, Liu X-W, Gong W-X, Sun X-F, Cui J-J, Gao B-Y. Interaction between congo red and copper in a binary adsorption system: Spectroscopic and kinetic studies. *Colloids Surf A*. 2009;340:86–92.
45. Klimaszewski K, Bald A, Sengwa RJ, Choudhary S. Static permittivities of ethanol mixtures with isomers of propanol and

butanol at temperatures from 288.15 to 308.15 K. *Phys Chem Liq*. 2013;51:532–546.
46. Seidel-Morgenstern A. Experimental determination of single solute and competitive adsorption isotherms. *J Chromatogr A*. 2004;1037:255–272.
47. Mohsen S, Shohreh F, Ali V. Mathematical modeling of single and multi-component adsorption fixed beds to rigorously predict the mass transfer zone and breakthrough curves. *Iran. J. Chem. Chem. Eng*. 2009;28:25–43.
48. Silva1 EA, Vaz LGL, Veit MT, Fagundes-Klen MR, Cossich ES, Tavares CRG, Cardozo-Filho L, Guirardello R. Biosorption of chromium(III) and copper(II) ions onto marine alga *Sargassum sp*. in a fixed-bed column. *Adsorpt Sci Technol*. 2010;28: 449–464.

Manuscript received Feb. 26, 2014, and revision received Sept. 13, 2014.